Wavefront reconstruction with pupil fragmentation: study of a simple case

Sylvain Bonnefond[a,b], Michel Tallon[b], Miska Le Louarn[a], and Pierre-Yves Madec[a]

[a]ESO, AOSY, Karl Schwarzschildstraße 2, D-85748, Garching, Germany
[b]Univ Lyon, Univ Lyon1, Ens de Lyon, CNRS, Centre de Recherche Astrophysique de Lyon UMR5574, F-69230, Saint-Genis-Laval, France

ABSTRACT

The use of smaller subapertures on some recent adaptive optics (AO) systems seems to yield difficulties in wavefront reconstruction, known as spider effect or pupil fragmentation: the size of the subapertures is small enough so that some of them are masked by the telescope spider, dividing the pupil into disconnected domains. In particular, this problem will arise on the E-ELT. We have studied pure wavefront reconstruction on a Shack-Hartmann wavefront sensor, for a simplified AO system similar to VLT/SPHERE in size, with and without pupil fragmentation, and compared the performance of various wavefront reconstructors for different signal-to-noise ratios, using priors (minimum variance) or not (least-squares), and with different assumptions for the damaged wavefront measurements. The missing measurements have been either discarded (corresponding subapertures are not active), replaced by zeros, or interpolated by preserving the loop continuity property of the gradients (curl operator). Priors have been introduced using the FrIM (Fractal Iterative Method) algorithm. In our perfect conditions, we show that no method allows the full recovery from the pupil fragmentation, that minimum variance always gives the best performance, especially the one without any interpolation. On the opposite, the performance with least-squares somewhat improves when correcting for the missing measurements. In this latter case, preserving the curl property of the gradient is preferable only for very low measurement noise.

Keywords: Adaptive optics, Wavefront reconstruction, Spider effect, SCAO system, Least-squares, Minimum Variance

1. INTRODUCTION

The use of smaller subapertures on some recent adaptive optics systems and the design of thick spiders on large telescopes yield difficulties in the wavefront reconstruction from Shack-Hartman wavefront sensor measurements. On these configurations, the width of the spider is no more negligible compared to the size of the subapertures and can hide full rows of subapertures. As a result, the spider divides the map of the measured wavefront gradients in disconnected domains, with missing or damaged gradient measurements between them. Unseen modes made of differential pistons between the disconnected domains are then created. This phenomenon is known as the spider effect or the pupil fragmentation, and has been clearly shown on EELT simulations[1] and could be the source of the so-called SPHERE low-wind effect.[2]

If the disconnected domains can be reconstructed independently, the reconstruction of the full wavefront surface needs to solve a cophasing problem from additional measurements sensitive to the phase differences between the domains. Of course another wavefront sensor sensitive to the phase, *e.g.* the pyramid wavefront sensor,[3] could overcome the fragmentation problem.

Before to consider alternatives, the aim of our study is to estimate the significance of the pupil fragmentation on the performances in the best conditions without adding other measurements, and to evaluate the behaviour of various solutions and reconstructors, only using the incomplete gradient measurements from a Shack-Hartmann wavefront sensor. The questions we want to address are: What is the best we can do with spider effect? Can a recovering be expected in the best conditions? How the effect depends on the measurement errors? Do we really need additional measurements?

As a basis of this study we use an inverse crime approach,[4] meaning that we use the exact same Shack-Hartmann wavefront sensor model for simulating the data as for the reconstructions, assuming that noise and turbulence statistics are perfectly known. Thus we consider pure open-loop reconstructions without any error like aliasing or fitting error, only assessing the effect of the measurement noise and of the pupil fragmentation.

Further author information: mtallon@obs.univ-lyon1.fr

We will consider both a minimum variance reconstructor taking priors on turbulence statistics into account[5] or a least-squares reconstruction with minimum norm,[6,7] with different ways to take the spider effect into account, as explained in section 2. Section 3 summarizes the parameters and assumptions of our simulations, and section 4 presents the results.

2. WAVEFRONT RECONSTRUCTION METHODS

We assume a linear direct model of a Shack-Hartmann wavefront sensor with Fried geometry:[8]

$$\boldsymbol{d} = \mathbf{S}.\boldsymbol{w} + \boldsymbol{n}\,, \tag{1}$$

where $\boldsymbol{d}$ is the vector of gradient measurements, $\mathbf{S}$ the wavefront sensor interaction matrix, $\boldsymbol{w}$ the vector of phase samples at the corners of the subapertures,[8] and $\boldsymbol{n}$ an additive *i.i.d.* gaussian noise with known variance σ_n^2 and zero mean. In the following, $\boldsymbol{d}$ and $\boldsymbol{n}$ are measured as optical path differences between the opposite sides of the subapertures, with the same units as the wavefronts $\boldsymbol{w}$. The wavefronts are then reconstructed from the data $\boldsymbol{d}$ using:

$$\widehat{\boldsymbol{w}} = \mathbf{R}.\boldsymbol{d}\,, \tag{2}$$

where $\mathbf{R}$ is the reconstruction matrix. Performances are estimated by computing the residual wavefront error σ_w with:

$$\sigma_w^2 = \frac{1}{N_w}\langle \|\widehat{\boldsymbol{w}} - \boldsymbol{w}\|^2 \rangle\,, \tag{3}$$

where N_w is the number of wavefront samples in the pupil.

The effect of the spider is simulated by discarding the measurements corresponding to the hidden subapertures.

Two reconstruction estimators

We consider and will compare the behavior of a minimum variance reconstructor and a least-squares reconstructor. The minimum variance reconstructor is the one derived by Thiébaut & Tallon 2010[5] for the Fractal Iterative Method (FrIM) algorithm, assuming here an *i.i.d.* additive noise, so that the covariance matrix of the noise is reduced to the identity matrix scaled by σ_n^2:

$$\mathbf{R} = (\mathbf{S}^{\mathrm{T}}.\mathbf{S} + \sigma_n^2\,\mathbf{K}^{-\mathrm{T}}.\mathbf{K}^{-1})^{-1}.\mathbf{S}^{\mathrm{T}}, \tag{4}$$

where $\mathbf{K}$ is the so-called fractal operator.[5] Note that the FrIM reconstructor can be expressed as a pre-calculated matrix, $\mathbf{R}$, it does not necessarily have to be iterative and using the original fast preconditioned conjugate gradient. The fractal operator $\mathbf{K}$ corresponds to a factorization of an approximate of the covariance matrix of the wavefront samples.[5] Since $\mathbf{K}$ is also used here for the simulation of wavefronts, the priors in Eq. (4) are exact.

The least-squares reconstructor is obtained using the minimum-norm maximum likelihood in zonal basis:[7]

$$\mathbf{R} = \lim_{\epsilon \to 0^+} (\mathbf{S}^{\mathrm{T}}.\mathbf{S} + \epsilon\,\mathbf{I})^{-1}.\mathbf{S}^{\mathrm{T}}, \tag{5}$$

The reconstructed wavefront with least-squares depends on the basis used to express the wavefronts. We will consider either the zonal basis that can be considered as the worse one since the cause of the fragmentation is very localized on the pupil, or the basis of the fractal modes that should be here the optimal one since it is the modes used to generate the turbulent wavefronts.

Four methods for dealing with the spider effect

The performance of the reconstructors are studied in the following four configurations:

No spider. The case without spider is our reference case with no missing data to assess the loss of performance caused by the spider effect.

No padding. In this case, the equations corresponding to the subapertures hidden by the spider are simply removed from the system. There is no attempt to replace the missing data. This method assumes that the reconstructor can be computed again if the hidden subapertures change, for instance due to a rotation of the spider during the observation.

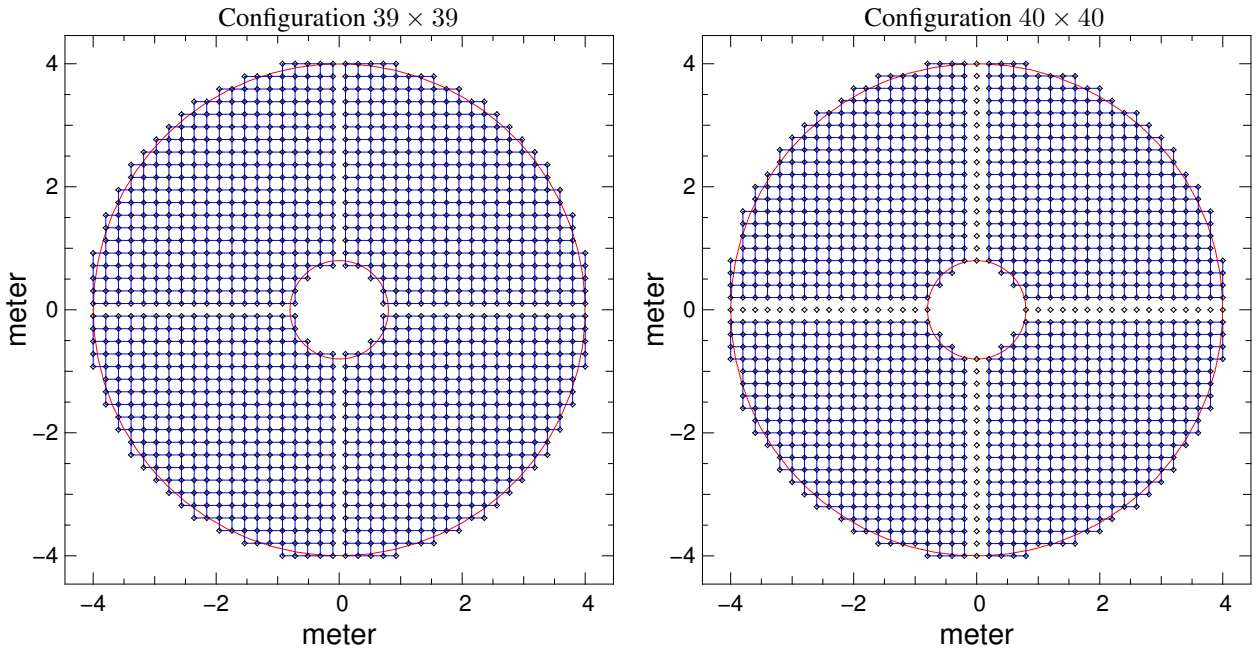

Figure 1. Considered configurations for an 8m telescope: 39×39 subapertures with a spider 1 subaperture in width (left) and 40×40 subapertures with a spider 2 subapertures in width (right) in order to assess the effects of the width of the hidden zones. Wavefront samples are plotted as circles (Fried geometry).

Padded with zeros. This case implicitely assumes that the reconstruction matrix cannot be recomputed so that all the expected data values must be given anyway. The missing data are simply replaced with zeros, enforcing the wavefront to be flat in its hidden parts. This strategy is a way to stitch the fragmented pieces of the wavefronts. This method sounds logical for an on-axis AO where the wavefront measurements are driven to zero by the system.

Padded with loops. This case is comparable to the previous one, but the missing data are here replaced with values as small as possible, but in agreement with the loop continuity property of the gradients, *i.e.* the sum of the gradients along any closed-path is equal to zero. The values are determined using the boundary method introduced by Poyneer et al. 2002[9] where a set of loop continuity equations are solved for all the smallest loops that involve missing data. The obtained values simply replace the missing ones in the set of data before applying the reconstruction matrix.

3. THE CONSIDERED CONFIGURATIONS

The performance of the reconstructors for the different cases presented in the previous section are assessed by numerical simulations for two close configurations with a spider 1 or 2 supabertures in width, for 39×39 and 40×40 supabertures respectively, as shown on Fig. 1. The spiders are introduced with a very simple straight geometry, so that no subaperture is partially hidden by the spider.

The simulations assume a 8m telescope with 20% central obscuration in diameter, and we consider von Kármán turbulence with a Fried parameter $r_0 = 17\mathrm{cm}$ and an outer scale $L_0 = 25\mathrm{m}$.

The model of the wavefront sensor is the same for the reconstruction and for the simulation (inverse crime[4]), so the performance only account for the open-loop reconstruction (*e.g.* no fitting error, no aliasing). It is measured as the rms (root mean square) difference between simulated and reconstructed wavefronts on the pupil, over 200 independent reconstructions. For each configuration case, we measure the errors from the reconstruction of the exact same series of 200 independent wavefronts.

The added noise is uniform and uncorrelated between measurements, and measured as the optical path difference between opposite sides of the subapertures. We will assess the rms error as a function of the level of noise, since the reconstructors have variable behaviors when the level of noise changes.

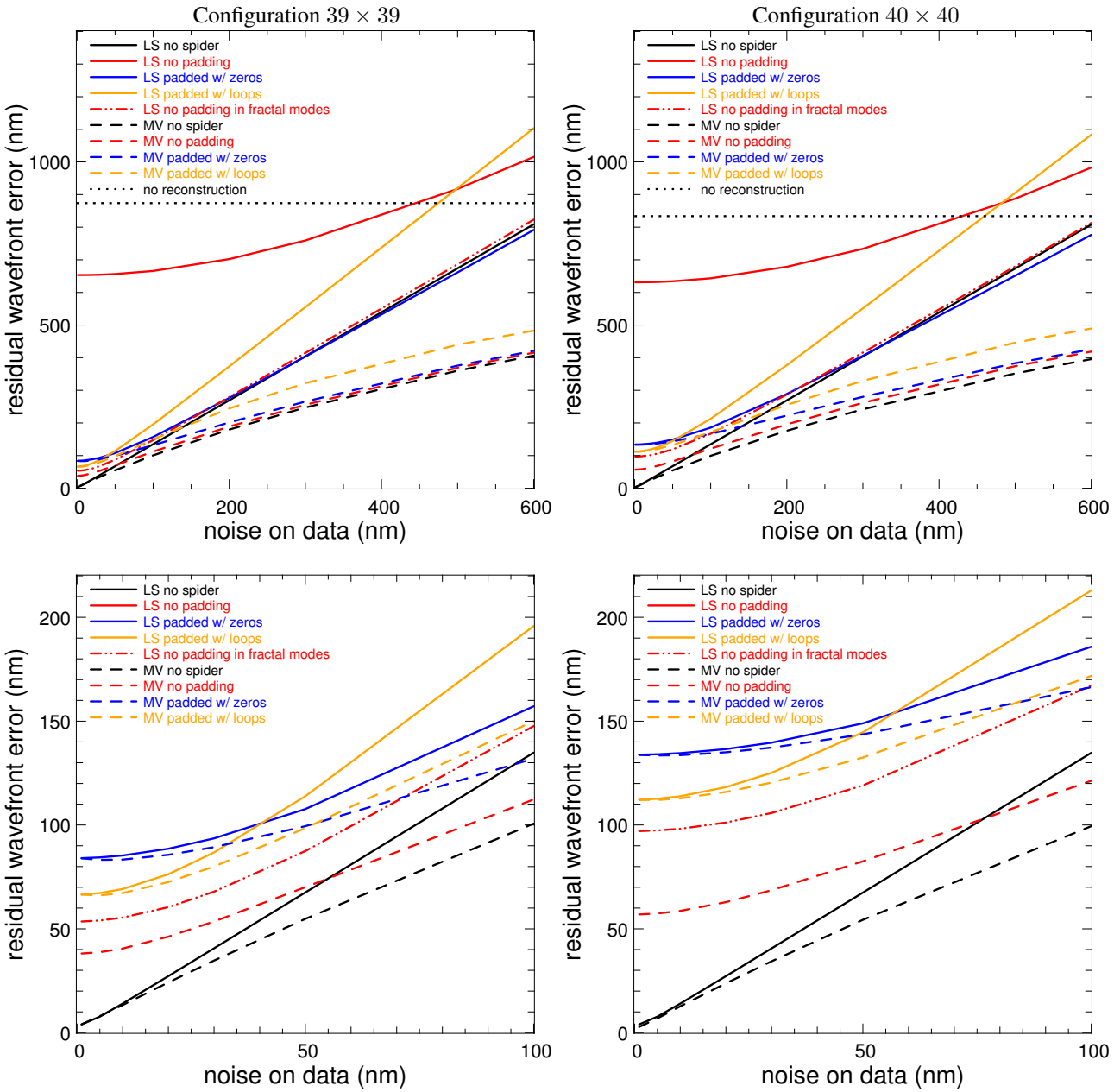

Figure 2. Residual wavefront errors in nm obtain for the configurations 39×39 (left) and 40×40 (right) shown in Fig. 1, for the various methods detailed in the text, using either least-squares with minimum norm (LS, solid curves) or minimum variance (MV, dashed curves). Bottom graphs are the same as the top ones, but plotted in the first 100nm range only. The dash-dot red curve gives the performance of LS reconstruction in the basis of fractal modes for the case no padding; all the other cases give the same curves as the ones for LS in zonal basis.

4. SIMULATION RESULTS

The results are summarized on Fig. 2. As expected, the errors are higher with a wider spider (39×39 on the left compared to 40×40 on the right), but the analysis that can be drawn out from these results is qualitatively the same.

No spider. The reference case is plotted in black in Fig. 2. Although the bias[7] (residuals with no noise), is similar between MV and LS for the 39×39 configuration it is slightly improved in the 40×40 configuration, from 4nm for LS to 2.8 nm for MV, because the priors can partially guess a greater number of unseen modes. The noise propagation is

higher for LS since no regularization (and no modal truncation) is introduced. In the "inverse crime" regime, MV gives the best performance we can expected.

No padding. In this case, the equations corresponding to the hidden subapertures are removed from the system. The results are plotted in red in Fig. 2. With this approach, MV reaches better performances than any other method for the recovery of the spider effect. Here, the wavefront fragments are stitched using the priors, *i.e.* with the best we can know from the modeling, including the loop continuity property of the missing measurements. Since MV minimizes the residual errors by construction, it is theoretically the best solution compared to any interpolation of the missing data. LS with zonal basis is the worst solution here. The four fragments of wavefront are reconstructed independently, piston removed in each one (minimum norm), so that they are far from being co-phased. On the opposite, LS in the basis of the fractal modes (dash-dot red curve), gives the best results for a large range of noise level (0-200 nm). The use of these modes somehow optimally guess the fragmented piston from the part of the modes seen by the wavefront sensor.

Padded with zeros. The results obtained by replacing missing measurements with zeros are plotted in blue in Fig. 2. The method is equivalent to setting priors where the measurements are missing. With MV, performances show that the information added by this correction is worse than relying on priors only, with a more significant degradation as the noise level decreases. For LS, zonal and fractal basis yield to the same performance, contrary to the case without padding. The performance are improved very significantly, but the bias is still strong (84 nm), significantly higher than without spider (4 nm), and than the best recovery that can be obtained with MV (38 nm). We can notice that this solution is better than the case LS with no spider for noise larger than 250nm, because less degrees of freedom are reconstructed, so the bias is larger and the noise propagation is lower.

Padded with loops. The results obtained by replacing the missing data with values as small as possible while preserving the loop continuity property of the gradients are plotted in orange in Fig. 2. The method has a similar effect than replacing missing data with zeros. With MV, performances show that the information added by this correction is again worse than relying on priors only. For LS, the results are again exactly the same with zonal or fractal basis. In any case, this approach is better than replacing by zeros for low noise (less than 40-50nm), but it is rapidly impeded by noise propagation.

5. CONCLUSION

The impact of a 1 or 2 subaperture thick spider is considerable on the wavefront reconstruction performance, even without noise. Some way of dealing with this effect has to be used. In the case of a LS reconstructor, the method preserving the loop continuity property works well, but propagates more noise. The best solution found here is a minimum variance reconstructor, which best solves the problem. Still, the performance without spider is never reached, even with the best reconstruction scheme.

In the 39x39 case, losing one row of subapertures of spider increases, without any noise contribution, the residual wavefront error by 38nm rms in the best case (minimum variance). In case of a LS reconstructor, this error is 68 nm rms. If nothing is done, in a LS case in a zonal basis, the wavefront error is a whopping 650 nm, severely handicapping the system performance. This underlines the severity of the pupil fragmentation problem, and shows that it must be dealt with. As another example, preliminary simulations on an E-ELT sized case (75×75 subapertures on a 39m telescope, spider 1 subaperture in width) show that the best performance we can obtain, with MV reconstructor and no noise, is 68nm rms.

Increasing the spider width to 2 sub-apertures makes the problem even more difficult to solve. Indeed, the best residual that can be obtained is now 58nm rms (whereas was 37 nm rms with a single subaperture width) using the minimum variance approach. With a pure LS reconstructor and loops constrain, this number is increased to 110 nm rms.

We can see that a thick spider is quite damageable to the AO system performance, even in the case of a minimum variance reconstructor, which is currently the best way to algorithmically solve the pupil fragmentation problem. Since the residuals tend to be non negligible with these approaches, new algorithms or probably a hardware solution should be investigated. For instance, a solution could use a pyramidal wavefront sensor which does not suffer from the unseen modes and could improve the performances of a telescope with a spider.

REFERENCES

[1] Le Louarn, M., Béchet, C., and Tallon, M., "Of Spiders and Elongated Spots," in [*Adaptive optics for Extremely Large Telescopes*], *3rd AO4ELT conference* (2013). Florence, Italy, May 26-31.

[2] Sauvage, J. F., Fusco, T., Girard, J., Milli, J., Bourget, P., Dohlen, K., L., B. J., and Mouillet, D., "Tackling down the low-wind effect with SAXO, the SPHERE eXtreme Adaptive Optics system," in [*Adaptive Optics Systems*], *Proc. SPIE* **9909** (2016).

[3] Vérinaud, C., "On the nature of the measurements provided by a pyramid wave-front sensor," *Optics Communications* **233**, 27–38 (2004).

[4] Colton, D. and Kress, R., [*Inverse Acoustic and Electromagnetic Scattering Theory*], Springer, Berlin (2013).

[5] Thiébaut, E. and Tallon, M., "Fast minimum variance wavefront reconstruction for extremely large telescopes," *Journal of the Optical Society of America A* **27**, 1046 (2010).

[6] Herrmann, J., "Least-squares wave front errors of minimum norm," *Journal of the Optical Society of America A* **70**, 28–35 (1980).

[7] Béchet, C., Tallon, M., and Thiébaut, É., "Comparison of minimum-norm maximum likelihood and maximum a posteriori wavefront reconstructions for large adaptive optics systems," *Journal of the Optical Society of America A* **26**, 497 (2009).

[8] Fried, D. L., "Least-square fitting a wave-front distortion estimate to an array of phase-difference measurements," *Journal of the Optical Society of America (1917-1983)* **67**, 370–375 (1977).

[9] Poyneer, L. A., Gavel, D. T., and Brase, J. M., "Fast wave-front reconstruction in large adaptive optics systems with use of the Fourier transform," *Journal of the Optical Society of America A* **19**, 2100–2111 (2002).